Available online at www.sciencedirect.com

SciVerse ScienceDirect

journal homepage: www.elsevier.com/locate/watres

Modeling transport of *Escherichia coli* in a creek during and after artificial high-flow events: Three-year study and analysis

A. Yakirevich [a], Y.A. Pachepsky [b,*], A.K. Guber [c], T.J. Gish [d], D.R. Shelton [b], K.H. Cho [e]

[a] Zuckerberg Institute for Water Research, J. Blaustein Institutes For Desert Research, Ben-Gurion University of Negev, Sede Boqer Campus, 84990, Israel

[b] USDA-ARS Environmental Microbial and Food Safety Lab., 10300 Baltimore Avenue, Building 173, Beltsville, MD 20705, USA

[c] Michigan State University, Dep. of Plant, Soil and Microbial Sciences, East Lancing, MI 48824, USA

[d] USDA-ARS Hydrology and Remote Sensing Lab., Beltsville, MD 20705, USA

[e] School of Urban and Environmental Engineering, Ulsan National Institute of Science and Technology (UNIST), 100 Banyeon-ri, Eonyang-eup, Ulju-gun, Ulsan 698-805, South Korea

ARTICLE INFO

Article history:
Received 6 September 2012
Received in revised form
2 January 2013
Accepted 7 February 2013
Available online 21 February 2013

Keywords:
Numerical modeling
Escherichia coli
Creek
Sediment
Resuspension
High-flow

ABSTRACT

Escherichia coli is the leading indicator of microbial contamination of natural waters, and so its in-stream fate and transport needs to be understood to eventually minimize surface water contamination by microorganisms. To better understand mechanisms of *E. coli* release and transport from soil sediment in a creek the artificial high-water flow events were created by releasing 60–80 m^3 of city water on a tarp-covered stream bank in four equal allotments in July 2008, 2009 and 2010. A conservative tracer difluorobenzoic acid (DFBA) was added to the released water in 2009 and 2010. Water flow rate, *E. coli* and DFBA concentrations as well as water turbidity were monitored with automated samplers at three in-stream weirs. A one-dimensional model was applied to simulate water flow, and *E. coli* and DFBA transport during these experiments. The Saint–Venant equations were used to calculate water depth and discharge while a stream solute transport model accounted for release of bacteria by shear stress from bottom sediments, advection-dispersion, and exchange with transient storage (TS). Reach-specific model parameters were estimated by evaluating observed time series of flow rates and concentrations of DFBA and *E. coli* at all three weir stations. Observed DFBA and *E. coli* breakthrough curves (BTC) exhibited long tails after the water pulse and tracer peaks had passed indicating that transient storage (TS) might be an important element of the in-stream transport process. Comparison of simulated and measured *E. coli* concentrations indicated that significant release of *E. coli* continued when water flow returned to the base level after the water pulse passed and bottom shear stress was small. The mechanism of bacteria continuing release from sediment could be the erosive boundary layer exchange enhanced by changes in biofilm properties by erosion and sloughing detachment.

Published by Elsevier Ltd.

* *Corresponding author*. Tel.: +1 301 504 7468; fax: +1 301 504 6608.
E-mail addresses: yakov.pachepsky@ars.usda.gov, yakov.pachepsky@gmail.com (Y.A. Pachepsky).
0043-1354/$ – see front matter Published by Elsevier Ltd.
http://dx.doi.org/10.1016/j.watres.2013.02.011

List of symbols

A	creek cross-sectional area, m^2
A_{st}	cross-sectional area of the storage zone, m^2
C	*E. coli* concentration in stream, MPN m^{-3}
C_b	*E. coli* concentration in streambed sediments, MPN kg^{-1}
C_g	*E. coli* concentration in groundwater, MPN m^{-3}
C_{st}	*E. coli* concentration in transient storage, MPN m^{-3}
c_d	drag coefficient
D	dispersion coefficient, $m^2\ s^{-1}$
f_{st}	storage ratio parameter
g	gravitational acceleration, m s^{-2}
h	height of water column (m)
H_b	streambed layer of a thickness, m
k_{dc}	bacteria die-off rate in water, s^{-1}
k_{db}	bacteria die-off/production rate in sediments, s^{-1}
MIA	modified index of agreement
n	bed roughness
NSE	Nash-Sutcliffe efficiency index
Q	creek discharge, $m^3\ s^{-1}$
q_g	groundwater flux to the creek per unit of creek length, $m^2\ s^{-1}$
R_e	entrainment coefficient, kg $m^{-2}\ s^{-1}$
R_d	*E. coli* deposition rate, m s^{-1}
R_r	*E. coli* resuspension rate, kg $m^{-2}\ s^{-1}$
S_F	friction slope
S_0	bed slope
t	time (s),
u	average flow velocity (m s^{-1}),
v_s	settling velocity, m s^{-1}
w	creek width, m
x	distance along creek (m)
α	stream-storage exchange coefficient, s^{-1}
ρ_b	sediment bulk density, kg m^{-3}
τ_b	bed shear stress, N m^{-2}
τ_{cr}	critical shear stresses for resuspension, N m^{-2}
τ_{cd}	critical shear stresses for deposition, N m^{-2}

1. Introduction

Microbial activity influences the safe use of surface waters for recreation, irrigation, aquaculture, husbandry, as well as for drinking and other household uses. Fecal bacteria like enterococci and *Escherichia coli* are commonly used to measure the sanitary quality of water and when in high numbers suggest an increased likelihood of bacteria pathogens which can adversely impact human health (Wade et al., 2006). *E. coli* can exist for up to several days in surface water or perhaps months in river and lake sediments, and it is the leading indicator of microbial contamination of natural waters (US EPA, 1986, 2003; Elmund et al., 1999; Garzio-Hadzick et al., 2010). There is a need to understand in-stream fate and transport of *E. coli* so as to understand and limit contamination of surface water by microbial organisms.

Runoff from manured fields and pastures, as well as direct deposition of animal waste to water are traditionally viewed as important sources of *E. coli* in rural watersheds (Jamieson et al., 2004). There is increased evidence that sediment resuspension during the high-flow events can detrimentally impact the microbial quality of recreation and irrigation waters (Pachepsky and Shelton, 2011). Recent studies indicate that sediments can harbor higher populations of fecal coliforms (FC) than the overlying water column (An et al., 2002; Muirhead et al., 2004). Consequently, Crabill et al. (1999) and Smith et al. (2008) have shown the importance of the monitoring sediment-borne *E. coli* for microbiological water quality studies during and after high-flow events.

Experiments with artificial high-flow events have been used in the past to distinguish the effect of resuspended sediment microbial releases from the effect of runoff microbial inputs. For example, water release from reservoirs (McDonald et al., 1982; Muirhead et al., 2004) or from tankers (Cho et al., 2010) to streams on rainless days has been used to simulate high water flows. In these studies, *E. coli* concentrations in water increased dramatically (up to two orders of magnitude) as the pulse of water passed the sampling station. The increases in *E. coli* were attributed to sediment resuspension and bacteria release.

Data from the artificial high-flow experiments demonstrate a very slow *E. coli* disappearance from water column after the high-flow events. Stable levels of *E. coli* and total coliform concentrations were observed by McDonald et al. (1982) for one hour after the pulse of water released from the reservoir passed the observation station. Similarly, in another experiment, high concentrations of about 2000 CFU per 100 ml was observed for two hours after the pulse of water from a supply reservoir had passed the observation stations 1.2 and 2.5 km downstream from the water supply reservoir (Muirhead et al., 2004). The high concentrations of *E.coli* perpetuating long after the water pulse passage could be interpreted as the result of a continued release of *E. coli* from the streambed. However, extended presence of high *E. coli* concentrations was also observed when the sampling location was relatively close to the water release location and the pulse was short enough to provide the fast return to the base flow after the pulse passage. For example, Cho et al. (2010) reported the presence of *E. coli* concentrations of about 1/3 of the maximum for two hours after the water pulse passage obtained at short distances of 130 and 260 m from the water release location. To explain the continuing *E. coli* presence, one had to assume that substantial release of bacteria from sediment continued in conditions close to base flow. Such an assumption seems to be dubious given the low *E. coli* concentrations in water column during base flow before the experiment, and exponential decrease of *E. coli* concentrations in sediment with depth (Pachepsky and Shelton, 2011).

A conceptual explanation of prolonged and elevated chemical and microbial concentrations after high-flow events in streams has been developed by analyzing transport of various solutes tracers through short sections of the stream networks (Gooseff et al., 2008). The explanation consists in formation of the transient storage (TS) which is filled during

the pulse passage and then gradually emptied thus providing a continuously working source of high chemical or microbial concentrations (Bencala and Walters, 1983; Gooseff et al., 2008). The existing frameworks for modeling bacteria transport in steams are based on advection-dispersion transport and sediment–water column interactions. Currently, models of sediment/bacteria transport in streams account for processes of resuspension and settling (Tian et al., 2002; Steets and Holden, 2003; Jamieson et al., 2005; Collins and Rutherford, 2004; Bai and Lung, 2005; Yang et al., 2008; Rehmann and Soupir, 2009; Cho et al., 2010; Russo et al., 2011). However, they disregard the effect of TS and therefore cannot simulate the long tails observed on the graphs of *E. coli* concentrations as a function of time or water flow. As a result, models with a term for TS need to be developed and evaluated to better understanding the release and transport of bacteria in streams.

The objectives of this work were: (1) to analyze results of three years (2008–2010) of artificial high and low flow experiments on a perennial first-order creek in a riparian zone; (2) to develop a numerical model of *E. coli* transport for the creek water as affected by resuspension, settling, and presence of transient storage; and (3) to assess inter-annual changes in *E. coli* transport parameters, and to elaborate on mechanisms of bacteria release and transport based on simulation results.

2. Materials and methods

2.1. Description of study area

The study site (Supplementary data, Figure S1) is located at the Optimizing Production Inputs for Economic and Environmental Enhancement (OPE3) watershed research site, USDA-Beltsville Agricultural Research Center on the mid-Atlantic coastal plain of Maryland. The entire watershed area is about 70 ha, with 75% employed in agricultural crop production while 15% is under deciduous forest. The site contains a small first-order creek (the Beaver Dam Creek Tributary described in detail by Angier et al., 2005) of ~1100 m long that is instrumented with four stations for monitoring stream flow and water sampling. The creek bed is from 100 to 160 cm wide and bed slope varies along the creek from 0.0008 to 0.0122 (Cho et al., 2010). The creek runs within a riparian corridor of variable width from about 65 m at its narrowest point, to more than 100 m. Four fields (A, B, C, and D in Figure S1, total area of 22.5 ha) have been under continuous corn production for the last 12 years. Field A receives 70,000 kg ha^{-1} dairy manure annually, whereas other fields receive only chemical fertilizers. Mean electrical conductivity and pH of water measured before and during experiment were 136 ± 58.2 μS cm^{-1} and 6.91 ± 0.35, respectively.

2.2. Sampling design and high-flow experiments

Four sampling stations located at 10, 150, 290 and 640 m from the water release point were instrumented with weirs and automated refrigerated samplers (Sigma 900 Max All Weather Refrigerated Sampler, Hach Company, Loveland, CO) to measure depth of water and to sample water in the creek (Figure S1). The weirs have been calibrated to convert depth of water to flow rate (Hively et al., 2006). The sections of the creek between stations 1 and 2, 2 and 3, and 3 and 4 are referred below as reach 12 (~140 m length), reach 23 (~140 m length), and reach 34 (~350 m length), respectively. The Trimble GeoXM 2005 Series global positioning system was used to determine elevations of the creek bottom at incremental distances along the creek. Creek sediment was sampled at 20-m increments along the creek to measure particle size distribution in the top 1-cm layer of the streambed. Fifty grams of sediment were collected at four positions across the creek at each sampling location to represent the texture variation across the stream.

Three artificial high-flow experiments were conducted on August 12, 2008, July 21, 2009 and July 20, 2010. In 2008 the creek sediment was sampled for *E. coli* concentrations at three locations downstream from stations 1, 2 and 4, while in 2009–2010 sediment was sampled equidistantly (every 20 m) in four replications within each reach 1 h before and one day after the high-flow event. Composite samples were taken across the creek from the top 2-cm layer of the streambed. The artificial high-flow event was created by releasing 60–80 m^3 of city water on a tarp-covered stream bank 10 m upstream from station 1 at a rate of around 60 L s^{-1} in four allotments (Table S1, Supplementary data). In 2009, 2010, a conservative tracer difluorobenzoic acid (DFBA) was added to the release water. Water was delivered in trucks, and time intervals between allotments (1 min, 3 min, and 1 min) were determined by truck logistics. The inlet pipe of the autosampler was placed on the bottom of the stainless steel weir. The weirs were cleaned before the experiment, so there was no sediment lying in the weir. Water samples were collected every 2 min at station 1, and every 5 min at stations 2, 3, and 4 while water depth in each weir was measured every minute.

2.3. Physical and microbiological analysis

2.3.1. Water

Water samples were transported to the laboratory on ice within 1 h and analyzed for *E. coli* concentrations using Colilert-18^{R} (IDEXX Laboratories, Inc., Westbrook, Maine) with Quanti-tray™/2000 trays (Olstadt et al., 2007). Five milliliters of the supernatant was added to IDEXX 100 mL bottles (two bottles per subsample for replication) containing 95 mL of sterile distilled water. One packet of Colilert-18 reagent was then added to each bottle and thoroughly shaken. After the reagent dissolved, bottle contents were poured into IDEXX trays and sealed with the IDEXX Quanti-Tray Sealer model 2X. The trays were then incubated at 37 °C for 18 h. To determine the Most Probable Number (MPN) of *E. coli*, positive, fluorescent wells within each Quanti-tray™/2000 tray were counted under 365 nm UV lighting (Spectroline CM-10, Spectro Corporation, Westbury, NewYork, USA). Turbidity was measured with the Orbeco-Hellige Digital Direct Reading Turbidimeter (Sarasota, FL). To quantify the DFBA tracer, a 3-mL aliquot from each sample was passed through a 0.2 μm filter and then analyzed by high performance liquid chromatography (HPLC) The HPLC conditions were as follows: mobile phase, acetonitrile 15 mM KH_2PO_4 (titrated to pH 2.6 with phosphoric acid (35:65, v/v) flow rate 1.7 mL min^{-1} guard column, Sperisorb

SAX1 (10 mm × 4.6 mm × 5-μm i.d., Waters Milford, MA); analytical column Supelcosil SAX (25 cm × 4.6 mm × 5-μm i.d., Sigma–Aldrich, St. Louis); injection volume 50 μL; and UV detection, 205 nm. The detection limit for DFBA was 50 μg L^{-1}.

2.3.2. Sediment

Sediment samples were scooped from the upper 1 cm of sediment, put into tubes with lids to prevent water loss, and immediately transported to the laboratory. The wet sediment and 90 mL of sterile distilled water were blended (blender model 34BL97, Waring) at high speed for 2 min in order to produce a homogeneous slurry (Garzio-Hadzick et al., 2010). After allowing the slurry to settle for 1 h, the supernatant was analyzed using the same procedure applied to water (Section 2.3.1). Note that potential IDEXX quantification errors due to particle-bound organisms have been previously explored by Fries et al. (2006) and determined to be minor in most scenarios. Sediment particle size was determined with the pipette method (Gee and Or, 2002). Sediment water content was determined in subsamples dried at 40 °C for 24 h. *E. coli* concentrations were expressed in MPN per gram of dry weight of sediment (gdw).

2.4. Flow and transport modeling

A one-dimensional model was applied to simulate water flow, *E. coli* and conservative tracer transport during the artificial high-flow events. The shallow water Saint–Venant equations were used to calculate water depth and discharge. The continuity and the momentum equations, respectively, are (Cunge et al., 1980):

$$\frac{\partial A}{\partial t}+\frac{\partial Q}{\partial x}=q_g \tag{1}$$

$$\frac{\partial Q}{\partial t}+\frac{\partial}{\partial x}\left(\frac{Q^2}{A}+gI_1\right)=gA(S_0-S_F)+gI_2+\beta q_g u \tag{2}$$

where A is the cross-sectional area (m^2), Q is the discharge ($m^3\ s^{-1}$), q_g is the groundwater flux to the creek per unit of creek length, ($m^2\ s^{-1}$), $S_F=n^2u|u|/h^{4/3}$ is the friction slope (–), n is bed roughness, S_0 is the bed slope (–), $g=9.8$ is the gravitational acceleration ($m\ s^{-2}$), $u=Q/A$ is the average flow velocity ($m\ s^{-1}$), $\beta\approx 1$ accounts for the effect of groundwater upwelling on momentum of flow, x is the distance along creek (m), and t is time (s),

$$I_1=\int_0^h (h-z)w(x,z)dz \text{ and } I_2=\int_0^h (h-z)\frac{\partial w(x,z)}{\partial x}dz \tag{3}$$

where h is height of water column (m) and w is the creek width.

For the simplicity we consider a stream of a rectangular cross-section of the width $W(x)$, then

$$I_1=Ah/2,\ \ I_2=bh^2/2 \tag{4}$$

where $b=\partial W/\partial x$.

The advection-dispersion equation is applied to simulate transport of *E. coli* and transport of a conservative DFBA tracer. The one-dimensional stream solute transport model accounts for advection-dispersion, lateral inflow/outflow, exchange with TS, linear die-off/production, and resuspension of bacteria from bottom sediments. Two approaches exist with respect to simulations of suspended bacteria transport (Russo et al., 2011). One approach assumes that bacteria are typically represented as "free" phase, or unattached to suspended sediments (Jamieson et al., 2004a) while the second approach assumes partitioning between "free" floating bacteria and those associated with suspended solids (Characklis et al., 2005; Bai and Lung, 2005). Often, a linear reversible adsorption isotherm is used describing microbe–sediment association (Russo et al., 2011). However, contradictory data exist with respect to the numbers of *E. coli* or FC associated with suspended sediments or between *E. coli* concentrations and turbidity (Pachepsky and Shelton, 2011). Also, introducing partitioning between "free" and "suspended sediments associated" phases into mathematical terms requires additional model parameters, which are difficult to determine and may increase uncertainty of predictions. Therefore, we assume that only one phase of *E. coli* is presented in the water column and their resuspension from bed sediments and settling is characterized by lumped parameters that can be estimated based on experimental data.

The governing equation of stream *E. coli* transport has a form

$$\frac{\partial(AC)}{\partial t}=\frac{\partial}{\partial x}\left(AD\frac{\partial C}{\partial x}\right)-\frac{\partial(QC)}{\partial x}-\alpha A(C-C_{st})+q_g^+C_g-q_g^-C+WR_rC_b-WR_dC-k_{dc}AC \tag{5}$$

where C and C_{st} are the *E. coli* concentration in stream and TS, respectively ($MPN\ m^{-3}$), D is the dispersion coefficient ($m^2\ s^{-1}$), α is stream-storage exchange coefficient (s^{-1}), R_r and R_d are *E. coli* resuspension ($kg\ m^{-2}\ s^{-1}$) and deposition rates ($m\ s^{-1}$), respectively, C_b is the *E. coli* concentration in streambed sediments ($MPN\ kg^{-1}$), C_g is the *E. coli* concentration in groundwater ($MPN\ m^{-3}$), $q_g^{\pm}=(q_g\pm|q_g|)/2$, and is k_{dc} the bacteria die-off rate in water (s^{-1}).

Exchange with TS (dead zones represented by stagnant pools, eddies etc.) is governed by a linear kinetic equation assuming first-order mass transfer (Bencala and Walters, 1983)

$$\frac{\partial(A_{st}C_{st})}{\partial t}=\alpha A(C-C_{st})-k_{dc}A_{st}C_{st}-h\upsilon_sC_{st} \tag{6}$$

where $A_{st}$is cross-sectional area of the storage zone (m^2), and υ_s is the settling velocity ($m\ s^{-1}$). Note that we neglect the bacteria release in TS zone. Since both the stream and the storage zone cross-sectional areas vary with time, a dimensionless measure of the storage effect is obtained by calculating the ratio of storage zone cross-sectional area to main channel cross-sectional area (Runkel et al., 1999). We assume that the storage ratio parameter, $f_{st}=A_{st}/A$, does not change with time, yet, it is reach specific.

The mass balance equation *E. coli* of in a streambed layer of a thickness H_b is

$$H_b\rho_b\frac{\partial C_b}{\partial t}=-R_rC_b+R_dC-k_{db}H_b\rho_bC_b \tag{7}$$

where k_{db} is the bacteria die-off/production rate in sediments (s^{-1}), and is ρ_b the sediment bulk density ($kg\ m^{-3}$).

The resuspension and deposition rates are calculated as (Russo et al., 2011):

$$R_r = \begin{cases} R_e(\tau_b/\tau_{cr} - 1) & \text{for } \tau_b > \tau_{cr} \\ 0 \text{ for } \tau_b \le \tau_{cr} \end{cases} \quad (8a)$$

$$R_d = \begin{cases} v_s(1 - \tau_b/\tau_{cd}) & \text{for } \tau_b < \tau_{cd} \\ 0 & \text{for } \tau_b \ge \tau_{cd} \end{cases} \quad (8b)$$

where R_e is the entrainment coefficient (kg m^{-2} s^{-1}), $\tau_b$is the bed shear stress (N m^{-2}), τ_{cr} and $\tau_{cd}$are critical shear stresses for resuspension and deposition, respectively (N m^{-2}).

The best estimate of the bed shear stress in a complex flow field can be obtained using the turbulent kinetic energy method (Biron et al., 2004). However this requires measurement fluctuations of the flow velocity components. Fairly good approximation of the average shear stress at the bed can be also obtained using the quadratic stress law, which relates stress to the square of the average fluid velocity (u) (Schlicting, 1987)

$$\tau_b = \rho c_d u^2 \quad (9)$$

where ρ is water density (kg m^3), and c_d is the drag coefficient. In our simulations we use average value of $c_d = 0.003$ (Cardenas et al., 1995).

The longitudinal dispersion is expected to increase with increasing discharge and flow velocity (Wallis and Manson, 2004), due to turbulence structures developing within the water column. Therefore we assume a linear dependence of the dispersion coefficient on flow velocity, as commonly accepted in porous media transport simulations (Bear, 1979), i.e. $D = au$, where a is the dispersivity (m).

To describe transport of a conservative tracer in a stream, we use Equations (5) and (6) assuming zero die-off/production rate, and resuspension-deposition processes.

For the Saint–Venant equations, the initial conditions define the distribution of water fluxes and water depth along the creek for base flow; while boundary conditions specify the value of flux (Neumann boundary condition) as a function of time at the stream inlet (for the supercritical flow, also the value of water depth is prescribed), and the transmissive boundary at the outlet (Neumann boundary condition). For the transport equation, the initial conditions define the concentration of *E .coli* and the tracer in the water and bed layer along the creek for base flow; while boundary conditions specify value of concentration in water column as a function of time (Dirichlet boundary condition) at the stream inlet, and the zero dispersive flux (Neumann boundary condition) at the outlet. The inlet boundary was assigned 10 m upstream of station 1, where water from trucks generated the high-flow events; and the outlet boundary was 10 m downstream of station 4.

The Saint–Venant equations were solved numerically by the finite volume method using a central-upwind scheme (Kurganov and Petrova, 2008) and the fourth order Runge-Kutta method with the estimate of truncation error (England, 1969) and the adaptive stepsize control (Press et al., 1992). The transport equations were solved by using implicit finite differences method and applying the front limitation algorithm (Haefner et al., 1997). The FORTRAN code was developed to implement numerical algorithm.[1] Benchmarking was performed using dam break solution (Stoker, 1957) for the Saint–Venant equations, and analytical solutions for the advection dispersion equation (van Genuchten and Alves, 1982).

[1] Available from the corresponding author by request.

2.5. Model fit procedure

Analysis of Beaver Dam Creek data relied on the trial-and-error approach. Reach-specific model parameters were estimated manually by using observed time series of water flow rates and concentrations of *E. coli* and DFBA at stations 2, 3 and 4. Any groundwater upwelling flux into the creek was calculated for each section of the creek between the weirs based on water balance as a difference between discharge at the reach outlet and inlet per unit length. Firstly, flow parameters were estimated by fitting simulated arrival time of artificially induced wave to the observed arrival time at a reach outlet. The bed roughness parameter (n) was changed consequently for each reach to fit the model simulations and observation. The second step was to estimate transport parameters: dispersivity (a), storage ratio (f_{st}) and exchange rate parameter (α) for each reach using DFBA breakthrough curves (BTCs). Calibration started from reach 12 by changing above three parameters for this reach, while holding values (initial guess) of these parameters at downstream reaches constant. When satisfactory agreement between observed and simulated BTCs at station 2 was achieved, this stepwise procedure was performed for each of the downstream reaches. Third step was to estimate parameters of bacteria resuspension using *E. coli* BTCs at stations 2, 3, and 4: the entrainment coefficient (R_e) and the critical shear stresses for resuspension (τ_{cr}). The critical shear stress for deposition was set as $\tau_{cd} = 0.8\tau_{cr}$, based on data of Russo et al. (2011). If a reasonable fit of *E. coli* BTCs was not achieved for the tested range of resuspension parameters values, then additional trial simulations were performed by modifying the storage ratio and exchange rate parameters initially found from DFBA tracer simulations.

The goodness-of-fit of the model was evaluated using the Nash-Sutcliffe efficiency index (NSE) and the modified index of agreement (MIA), as given by Legates and McCabe (1999):

$$\mathrm{NSE} = 1 - \frac{\sum_{i=1}^{N}(P_i - O_i)^2}{\sum_{i=1}^{N}(O_i - \overline{O})^2} \quad (10)$$

$$\mathrm{MIA} = 1 - \frac{\sum_{i=1}^{N}|P_i - O_i|}{\sum_{i=1}^{N}|P_i - \overline{O}| + \sum_{i=1}^{N}|O_i - \overline{O}|} \quad (11)$$

where P_i and O_i represent the simulated and observed values of state variables (head, concentration), $\overline{O}$ is the mean of O_i and is N number of observation. Values of NSE between 0 and 1 are generally viewed as acceptable level of model performance. Following Köhne et al. (2005) we consider simulations with MIA >0.75 as being "accurate".

3. Results and discussion

3.1. Sediment composition

The distributions of sediment particle fractions (clay + silt) at bottom along the creek in 2008–2010 are shown in Figure S2

(Supplementary data). Sediment was predominantly sandy at reach 12; the amount of silt and clay were generally higher in reaches 23 and 34. The percentage of clay and silt was variable with the smallest being observed in 2010. After the high-flow event the percentage of clay and silt slightly decreased in reach 12 and in the first half of reach 23 (Fig. S2b and S2c), while toward the end of reach 23 a decrease of clay and silt particles was observed. Percentage of clay and silt particles predominantly decreased along reach 34 after high-flow events. The significant increase in percentage of clay and silt particles occurred at the end of reach 23 in 2009 and along all creek length in 2010. Variations in sediment particle size along the creek are at least partially attributable to the channel slope of the creek (Cho et al., 2010). The relative contents of clay and silt were greatest in sites where the channel slope was lowest.

E. coli concentrations in the sediment along the creek one day before and one day after high-flow event are shown in Figure S3 (Supplementary data). The results illustrate that *E. coli* concentrations can vary substantially within relatively short distances. The spatial variability of *E. coli* and FC concentrations has often been attributed to the differences in sediment particle size distributions. For example, association of *E. coli* with clay and silt particles has been shown to be stronger than with sand particles (Guber et al., 2007; Pachepsky et al., 2006). Regression analysis has confirmed a significant direct relationship between the percentage of clay and silt particles and FC and *E. coli* concentrations in estuarine and riverine sediment samples from Northern California (Atwill et al., 2007). Garzio (2009) observed an increase in sediment *E. coli* concentrations with increasing silt content in the sediment of the creek where our experiments were conducted. On the other hand, Doyle et al. (1992) did not find a significant relationship between sediment coliform concentrations and sediment textural fractions contents; but in their case sediments were very coarse (>90% sand and gravel) and might not have provided a sufficient range of particle sizes to establish a relationship. In our study, the bacteria concentrations in sediment 2 h after the high flow event was initiated were smaller than just before the water release event and then significantly increased one day afterwards.

Distributions of *E. coli* in sediment and their resuspension can be influenced by the thickness of the sediment layer being disturbed by the high water-flow event. Results demonstrate that sediment *E. coli* content exhibits the power law dependence on the distance from the sediment surface with highest value in upper 1 cm of bed sediments (Pachepsky and Shelton, 2011). Alm et al. (2003) observed a twofold decrease in *E. coli* content in beach sand with 5 cm increments of depth within the first 15 cm. The coefficient of variation was about 30% and did not change with depth. Concentrations of FC in the top 2 cm of sediments were significantly ($p < 0.001$) higher than in the 2–10 cm layer (Ferguson et al., 1996).

3.2. *Flow modeling*

Table 1 shows the parameters associated with the flow model along with model goodness-of-fit indices. The most substantial addition of groundwater flux to creek flow occurred in reach 23. This is in agreement with the results of the study by Angier et al. (2005), who found a small (4.8 m^2) upwelling area that comprised only about 0.006% of the total riparian area (or approximately 0.001% of the entire catchment), yet supplied on average 4% of total stream flow.

The calibrated values of the roughness coefficient (Table 1) were between 0.06 and 0.15 and generally decreasing downstream. These values are consistent to those reported for some streams, e.g., $n = 0.11$ for Cypress Creek (Arcement et al., 1979) or $n = 0.12$ for Yockanookany River (Colson et al., 1979), but they were 2–3 times greater than the values reported by Chapra (1997). Inter-annual changes of the roughness coefficient are of order 10–20%, except reach 23 (Table 1), for which roughness estimates were almost half as large in 2009 because of the much earlier arrival time (by around 4 min) of the water pulse compared to that in 2008 and 2010. Channel geometrical irregularities, various obstructions to flow caused by riparian vegetation and large wooden debris that were present in the creek, can increase roughness (Chow, 1959). Additionally, one cannot exclude some effect of the weirs at the sampling stations on the water flow (Cho et al., 2010).

Fig. 1 shows the observed and simulated hydrographs at the three weir stations. Interruptions in water release caused several rising and falling limbs at the stations hydrographs with amplitude decreasing with distance. Although only roughness coefficient values were calibrated by fitting wave arrival times, the predicted flow rates were mostly in accordance with observed values. The values of NSE and MIA goodness of fit criteria (Table 1) indicated that the Saint–Venant equations simulated creek water flow accurately. The largest disagreement with the flow model was observed at station 2 in 2010 when simulated maximum values of water discharge were almost twice as large as those observed. However, the observed discharge at this station was significantly smaller than discharge at the creek inlet during water dumping. The discharge increased at stations 3 and 4 which was consistent with the simulation results. It is possible that flow can partly bypass this weir due to bank destruction. The model simulates rising limbs of the hydrographs better than falling ones which became less steep as the water pulse moved along the creek. We speculate that the relatively long tails could be attributed to rising pressure head making water move from the creek into the creek bank during the water wave arrival, and seeping back into to the creek after the water wave passed. This process is not accounted for by the Saint–Venant equations.

3.3. *Conservative tracer (DFBA) transport*

Fig. 2 presents comparison between observed and simulated BTCs of DFBA tracer. In 2009 the tracer was added to the creek with first water load, while in 2010 the tracer was added with first and third water loads (Table S1). As a result, two concentration peaks appear in 2010 (Fig. 2b). The observed BTCs exhibit long tails which means that TS could be an important mixing mechanism (Bencala and Walters, 1983). A fairly good agreement was obtained between observed and simulated BTCs of DFBA where the DFBA recovery was between 85% and 100% of that applied. For most BTCs calculated NSE and MIA indexes indicate that the model can be considered as a “good” predictor (Table 2). Most deviations between observation and model simulations occurred at station 4 for both 2009 and

Table 1 – Estimated flow model parameters and goodness of fit indexes for the Beaver Dam Creek Tributary.

Year	2008			2009			2010		
Reach	12	23	34	12	23	34	12	23	34
Groundwater flux, $q_{gw} \times 10^6$ m^2 s^{-1}	4.60	18.0	−0.05	15.7	6.37	1.15	2.62	16.2	0.88
Manning's roughness, n	0.15	0.13	0.10	0.14	0.06	0.08	0.13	0.12	0.08
Nash-Satcliffe efficiency, NSE	0.812	0.576	0.838	0.625	0.774	0.599	0.171	0.513	0.828
Modified index of agreement, MIA	0.910	0.817	0.924	0.823	0.887	0.805	0.699	0.772	0.926

2010. The MIA value of these BTCs are slightly below accepted critical value of 0.75 (Table 2, reach 34), yet according to NSE index the model performs well in simulations. The disagreement between observed and simulated tracer concentrations could be due to several issues. First, reach 34 is longest (~340 m) in the Beaver Dam Creek Tributary, and there is a possibility that the representative parameters values in the reach do not fall between representative values of its sub-reaches (Ge and Boufadel, 2006). This is important because TS and mixing processes depends on hyporheic exchange and groundwater inflows which are heterogeneous in both time and space (Gooseff et al., 2008). Second, we applied a TS model which represents exchanges between the main channel and a single storage zone, essentially lumping together different exchange processes. Briggs et al. (2009) developed a model that accounts for two storage zones: the surface transient storage (STS) and the hyporheic exchange transient storage (HTS). This approach sounds more physically based, yet their method to discriminate between two storage zones requires the determination of cross-sectional stream velocity distributions and stream tracer concentration time series data from several main channel locations adjacent to the representative STS zones. Finally, discrepancies between observed and model simulations may also be due to the trial-and error parameter estimates method that were used, while solving the inverse problem with optimization algorithms results in an improved simulation (Scott et al., 2003).

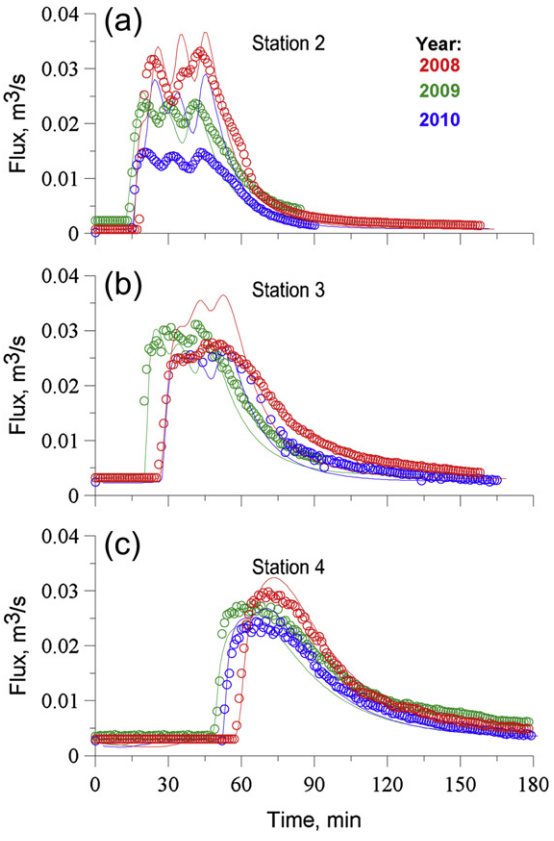

Fig. 1 – Flow rates during an artificial high-flow event in 2008 (red), 2009 (green) and 2010 (blue) at three monitoring stations 2, 3, and 4, respectively (a), (b) and (c). Open circles – observed, lines-simulated. (For interpretation of the references to color in this figure legend, the reader is referred to the web version of this article.)

Parameters for the DFBA transport simulations found by trial-and-error for three reaches are presented in Table 2. It should be understood that we adopted a linear approach for relating the dispersion coefficient to the flow velocity. Obtained values of dispersivity are in the range of 0.5–0.9 m, which means that in the simulated experiment the dispersion parameter varied from 0.013 to 0.12 m^2 s^{-1} for the base flow and then increased to 0.35 m^2 s^{-1} for the high-flow event. For the same creek, Cho et al. (2010) using *E. coli* accumulated mass BTCs found $D = 0.56$ m^2 s^{-1}, however their model did not account for TS exchange, which explains the larger D values. Our D values are consistent with those found in the literature. For example, in tracer experiments in Uvas Creek, Santa Clara County, California, Bencala and Walters (1983) determined D = 0.1–0.4 m^2 s^{-1} Scott et al. (2003) using same data and automated calibration adjusted D values to 0.01–0.2 m^2 s^{-1} Harvey et al. (1996) applied the Transient Storage Model (Bencala and Walters, 1983) to experimental results at St. Kevin Gulch, Colorado and estimated D values of 0.25 and 0.35 m^2 s^{-1} for low and high base flow, respectively.

Similar values of TS ratio parameter, f_{st}, were found in 2009 and 2010 (Table 2): 0.2 for reaches 12 and 23, and 0.1 for reach 34, which indicates a relative decrease in importance of the storage exchange along the creek. The exchange rate parameter, α, varies in a range from10^{-4} s^{-1} to 6×10^{-4} s^{-1} while the inter-annual variations of DFBA transport parameters were not substantial.

The TS slows down the movement of solutes relative to that expected from advection and dispersion processes alone (Runkel, 2002). A wide range in the distribution of transient-storage times within any given stream reach should be expected, ranging from small pools or eddies, that retain water and solutes for only a few seconds, to off-channel wetlands or long hyporheic flowpaths where stream water may be retained for days or weeks (Gooseff et al., 2008). Values of transient storage parameters found for tracer experiments in different locations vary in wide ranges of f_{st} = 0–3.0,

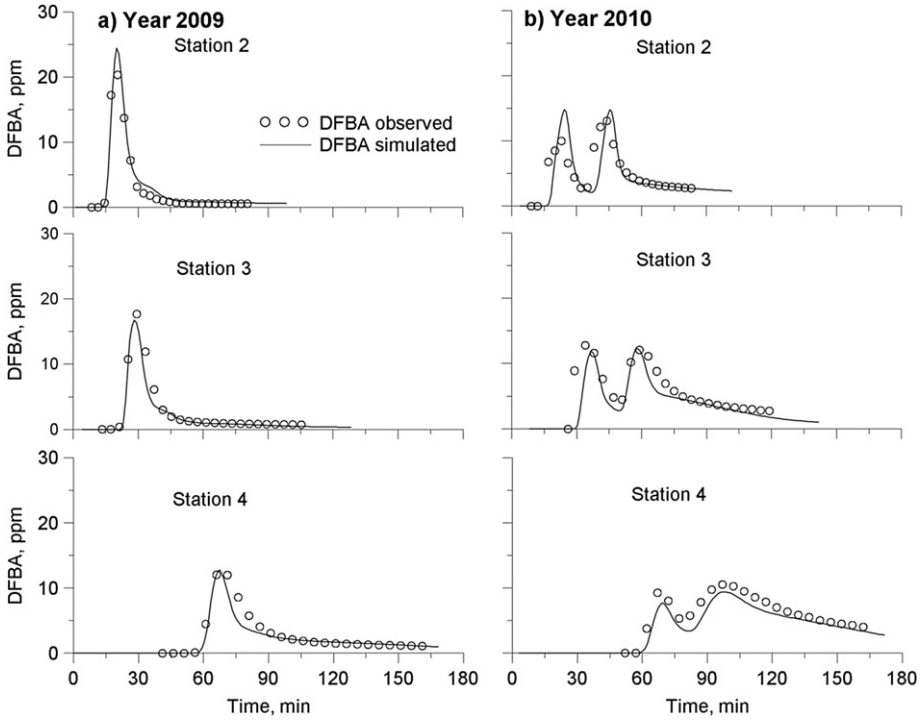

Fig. 2 – Observed and simulated BTCs of DFBA tracer at three stations in the Beaver Dam Creek Tributary in (a) 2009 and (b) 2010.

$\alpha = (1–4.5)\cdot10^{-5}$ s^{-1} (Bencala and Walters, 1983), $f_{st} = 0.16–0.92$, $\alpha = (2.5–7.8)\cdot10^{-5}$ s^{-1} for the same creek (Scott et al., 2003), $f_{st} = 1.82$ and 0.07, $\alpha = 0.82\cdot10^{-4}$ and $4.0\cdot10^{-4}$ s^{-1} for low and high base flow (Harvey et al., 1996).

3.4. E. coli *transport*

Fig. 3 shows turbidity, and observed and simulated *E. coli* concentrations at three creek stations during the high-flow events in 2008–2010. Turbidity and *E. coli* concentration BTCs at all stations were typical for the advective-dispersive type transport, having the bell shape and long tails indicative for the coupled TS effect and low rates of settling caused by re-entrainment of the sediment and associated *E. coli*. The tail concentrations were far above the regulatory threshold for *E. coli* concentrations signifying microbial impairment. *E. coli* BTCs had relatively narrow peaks, generally thinner than the peaks of hydrograph (Fig. 1) and turbidity (Fig. 3). This indicates that most significant bacteria resuspension occurred during first two water loads, while sediment resuspension continued. Most often turbidity peaked prior to *E. coli* concentrations and returned to lower levels more rapidly than *E. coli*. Turbidity and *E. coli* were only weakly correlated. Both strong and weak correlations between bacterial concentrations and turbidity have been reported in the literature. Muirhead et al. (2004) during artificial flood experiments observed that *E. coli* concentrations peaked ahead of the water flow peak, consistent with the entrainment of FC into the water column from underlying contaminated sediments and that *E. coli* concentrations were highly correlated with turbidity over the flood event ($R^2 = 0.92$). However, while the turbidity returned to base levels between each flood event, the *E. coli* concentrations remained somewhat elevated. On the other hand, McDonald et al. (1982) and Goyal et al. (1977) observed only a weak relation between *E. coli* concentration and turbidity.

Bacterial peak concentrations in 2009 were more than twice that of 2008 and around five times higher than in 2010. Spatially, the largest microbial concentrations were from reaches 12 and 23 while relatively small *E. coli* amounts were released from the sediments in reach 34. The differences in resuspension could be explained by the stronger association of bacteria with silt and clay sediment particles as compared with sandy particles. Sediment was predominantly sandy

Table 2 – Estimated parameters of DFBA tracer transport and goodness of fit indexes for the Beaver Dam Creek Tributary.

Year	2009			2010		
Reach	12	23	34	12	23	34
Dispersivity, *a*, m	0.9	0.7	0.5	0.6	0.9	0.7
Transient storage ratio, $f_{st} = A_{st}/A$	0.2	0.2	0.1	0.2	0.2	0.1
Exchange rate, $\alpha \times 10^4$, s^{-1}	4.0	2.0	1.0	6.0	3.0	2.0
Nash-Satcliffe efficiency, NSE	0.813	0.839	0.477	0.663	0.412	0.447
Modified index of agreement, MIA	0.905	0.915	0.730	0.841	0.752	0.728

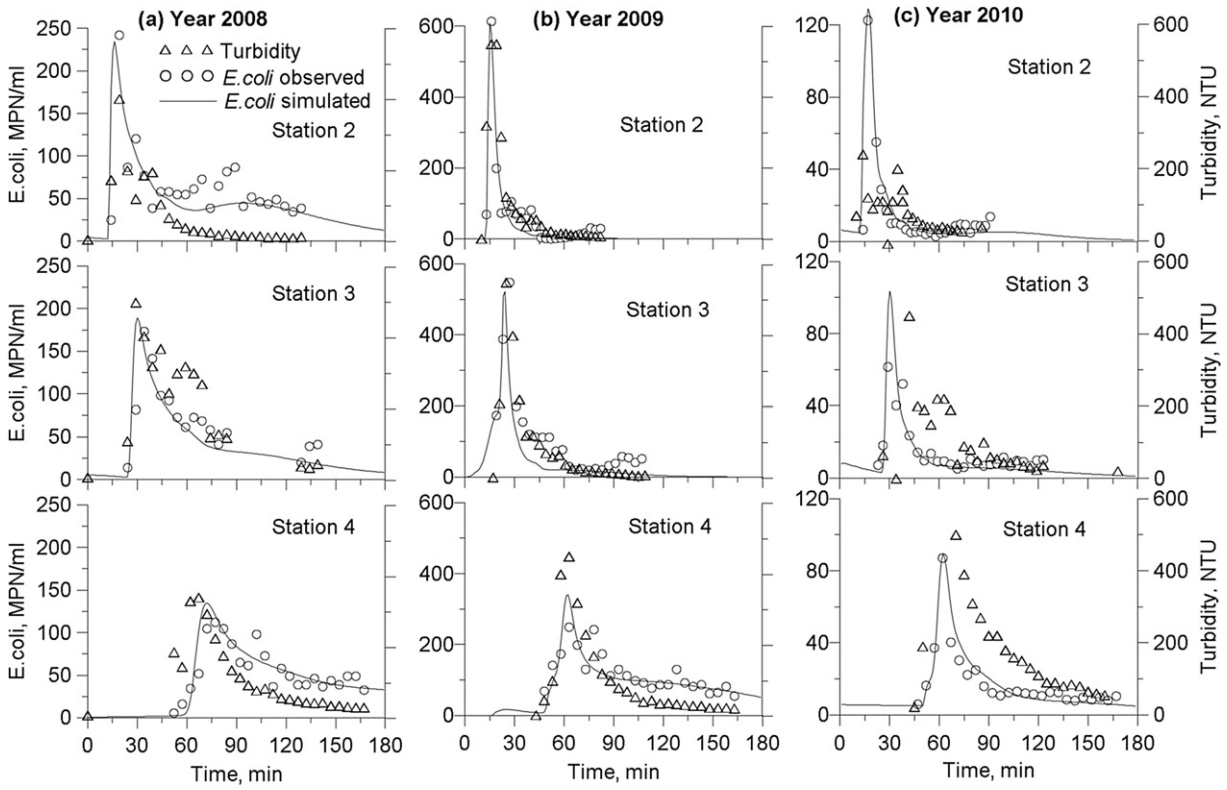

Fig. 3 – Observed turbidity, *E. coli* and simulated BTCs of *E. coli* at three stations in the Beaver Dam Creek Tributary in (a) 2008, (b) 2009 and (c) 2010.

upstream from station 1, and between stations 1 and 2, while the amount of silt and clay gradually increased from station 2 to 4. The percentage of clay and silt particles was large in 2008 and 2009 and fairly small in 2010 (Figure S2).

Model parameters estimated by fitting simulated and observed concentrations are presented in Table 3. In these simulations, a constant value of the settling velocity $v_s = 2.2 \cdot 10^{-6}$ m s^{-1} was accepted for clay particles (Russo et al., 2011), taking into account that the model sensitivity to this parameter was very low due to the observation time being relatively short (Cho et al., 2010). The bulk density and thickness of the bed layer where *E. coli* is subject to resuspension were respectively $\rho_b = 1500$ kg m^{-3} and $H_b = 0.01$ m. The zero rate of bacteria die-off/production was assumed, again due to the relatively short observation time (Cho et al., 2010).

Simulating *E. coli* transport with TS parameters determined for DFBA data did not provide a satisfactory fit to experimental *E. coli* BTCs, specifically at their tailings when the entrainment rate and critical share stress were varied in realistic ranges from 10^{-5} to 10^{-2} kg m^{-2} s^{-1} and from 0.01 to 0.5 N m^{-2}, respectively (results not shown). The transient storage volume computed from tracer concentration data simply was not large enough to store *E. coli* amounts sufficient to support long tails at *E. coli* BTCs. Therefore we had to either assume that TS volumes were different for *E. coli* and tracer or assume that TS volumes are the same but there is an additional mechanism supplying *E. coli* to the stream. We chose the former assumption. To implement it, the entrainment rate (R_e) and critical share stress (τ_{cr}) were estimated the using the rising portion of BTCs, then the initial TS parameters (estimated using DFBA) were changed to fit the BTC tails. Several iterations by changing resuspension and TS parameters were repeated until reasonable agreement was achieved. Additionally, model parameters for the thickness of bed layer

Table 3 – Estimated *E. coli* transport parameters and goodness of fit indexes for the Beaver Dam Creek Tributary.

Year	2008			2009			2010		
Reach	12	23	34	12	23	34	12	23	34
Transient storage ratio, $f_{st} = A_{st}/A$	0.5	0.15	0.2	0.3	0.5	0.4	0.2	0.2	0.1
Exchange rate, $\alpha \times 10^4$, s^{-1}	4.0	1.0	0.3	7.0	5.0	3.0	1.5	1.0	0.5
Critical shear stress, τ_{cr}, N m^{-2}	0.02	0.06	0.06	0.02	0.03	0.02	0.01	0.06	0.05
Entrainment rate, $R_e \times 10^3$, kg m^{-2} s^{-1}	6.0	2.0	0.6	65.0	23.0	4.0	2.8	0.1	0.8
Nash-Satcliffe efficiency, NSE	0.019	0.346	0.484	0.594	0.327	0.443	0.554	0.412	0.798
Modified index of agreement, MIA	0.590	0.726	0.760	0.817	0.667	0.722	0.804	0.752	0.903

subject to resuspension for reaches 12 and 23 in 2009 was increased from 1 to 2 cm. This increase in bed thickness was necessary to satisfy *E. coli* mass balance considerations. The estimated critical shear stress values vary from 0.02 to 0.08 N m^{-2} (Table 3), which is close to the values assessed by Cho et al. (2010) with experimental data from 2008. Differences in sediment properties can cause large differences in parameters that are important for predicting resuspension of *E. coli* from streambeds. For example, considerable differences have been found in the values of the critical shear stress defining the onset of resuspension in the modeling work on *E. coli* transport. Jamieson et al. (2005) reported the value of 1.7 N m^{-2}; Bai and Lung (2005) have used the value of 0.4 N m^{-2}, whereas significantly lower values of 0.02–0.1 N m^{-2} reported in the work of Steets and Holden (2003), 0.02 N m^{-2} (Lee et al., 1994), 0.031–0.132 N m^{-2} (Lau and Droppo, 2000) and 0.06–0.1 N m^{-2} (Droppo et al., 2007).

The entrainment rate coefficient varied in a range from 10^{-4} to 65 × 10^{-3} kg m^{-2} s^{-1} (Table 3) with highest values for reaches 12 and 23 in 2009. This parameter is sensitive to the peak concentration value that was very different among the three years of the study (Fig. 3). The inter-annual differences among *E. coli* concentrations in sediment (Fig. 2 in supplementary material) were not as pronounced as the peak concentrations (Fig. 3). Sediment and bacteria resuspension parameters can be affected by a biofilm developing in stream sediments. Gerbersdorf et al. (2008) found strong correlation of the colloidal and bound EPS moieties with the critical shear stress for erosion over sediment depth. Biostabilization and consolidation time act as a mechanisms for increasing the bed sediment stability and influencing erosion characteristics (Droppo et al., 2007; Stone et al., 2011).

In most simulations both NSE and MIA indexes indicate god model fit (Table 3). The worst agreement is observed for station 2 in 2008, yet the NSE index is positive indicating that at least qualitative behavior of released *E. coli* transport is described correctly by the model, as seen in Fig. 3a. Lower values of goodness of fit indexes for bacterial transport simulations can be attributed to more significant scattering of measured *E. coli* concentration compared to that of DFBA.

Fig. 4 shows calculated spatio-temporal variations of *E. coli* resuspension rate (R_rC_b). The resuspension rate depends on the water velocity because shear stress is a function of flow velocity, and on the distribution of bacteria concentrations in bed sediments. The non-uniform distribution of the flow velocity and initial bacteria concentrations in sediment resulted in patchy patterns of *E. coli* resuspension. The flow velocity was highest at distances 110–250 m from station 1 because of the larger stream bed slopes. Consequently, the *E. coli* resuspension rate was the largest in 2008 and 2009. Relatively low *E. coli* resuspension was estimated at the reach 34 in 2008 and the reach 23 in 2010 because of smaller mean concentrations in the initial bed sediments.

Fig. 4 shows that, in general, *E. coli* resuspension occurred at times between wave rising and falling limbs. A steep-frontal wave can effectively suck organisms from the bottom sediment and hold them in the turbulent wave front, while less steep front or falling wave can lift organisms but not draw them in the wave overrun (Wilkinson et al., 2006). After the water wave has passed and flow returned to steady

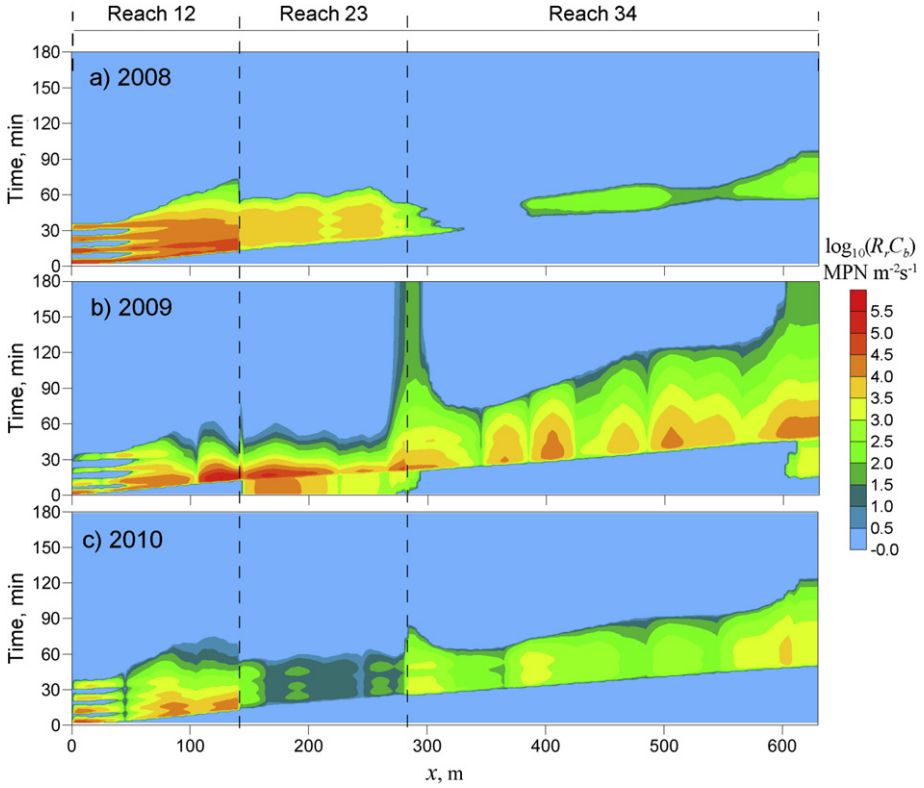

Fig. 4 – Spatio-temporal patterns of calculated *E. coli* resuspension rate due to mechanical disruption under artificial high-flow event in a) 2008, b) 2009, and c) 2010. Horizontal axis is the distance from monitoring station 1.

levels, the calculated shear stress was smaller than the critical one and the calculated rate of *E. coli* release from sediment was zero. Yet, observed *E. coli* BTCs exhibit elevated concentration of bacteria in the water column (Fig. 3).

The improved model fit was obtained by increasing values of the TS ratio compared to values of this parameter initially estimated using the DFBA tracer data. If one assumes that TS volumes are not related to the nature of the dissolved or suspended substance, then the TS volumes should be the same for the DFBA and *E. coli*, and some additional mechanisms exist that create elevated *E. coli* concentrations long after the water pulse passage. The mechanisms of *E. coli* release that were not accounted for in this work include: 1) the steady-flow stochastic erosion of bed and bank sources, resulting from high-flow turbulence (Wilkinson et al., 2006; Grant et al., 2011); 2) boundary layer exchange of bacteria trapped in streambed pore spaces by diffusion and/or quasi-periodic sweep and eject motions associated with coherent turbulence; and 3) hyporheic exchange which involves the release of bacteria trapped in streambed pore spaces by the advective flux of water across the sediment–water interface (Grant et al., 2011). Grant et al. (2011) measured the flux of fecal bacteria across the sediment–water interface in a turbulent stream (Riverside Wastewater Treatment Plant stream in southern California) at steady flow conditions. They found that bacteria release from sediment due to the first two mechanisms mentioned above were minor compare to that induced by hyporheic exchange which controls the transport of bacteria. The hyporheic exchange is accounted for in simulations by exchange bacteria in stream water with TS. Yet, *E. coli* release due to the steady-flow stochastic erosion of bed can be enhanced due to changes in macro-scale viscoelastic and other constitutive properties influencing biomass structure (Alpkvist and Klapper, 2007). Once the critical bed shear stress is surpassed sloughing of biofilms and further transport of bacteria occurs (Droppo et al., 2007, 2009). Thus, the term responsible for bacteria resuspension (R_b) during and after high-flow can be modified as follows

$$R_b = R_r C_b + k_e \rho_b C_b H(t - t_{cr}) \quad (12)$$

where k_e is the mass transfer rate due to enhanced erosive exchange (m s^{-1}), $H(t)$ is the Heaviside step-function and t_{cr} is time when the critical bed shear stress is surpassed. Application of Equation (12) for modeling *E. coli* release and transport in a creek is the subject of future research. We speculated that this hypothesis might help in resolving discrepancies between TS volumes estimated for conservative tracer and bacteria transport to the same extent or better than hypothesis about different TS volumes for *E. coli* and DFBA. However, we did not implement Equation (12) since we felt that additional experimental data should be collected to distinguish between the two hypotheses.

4. Conclusion

1. A mathematical model of bacteria release from bed sediment and subsequent transport in a stream under non-steady flow condition was developed and applied for simulation and analysis of DFBA tracer and *E. coli* transport during artificial high-flow experiments performed in 2008–2010 at the Beaver Dam Creek Tributary located on the mid-Atlantic coastal plain of Maryland.
2. The observed DFBA and *E. coli* BTC exhibited long tails after the water pulse and tracer peaks had passed indicating that TS might be an important element of the in-stream transport process. Fairly good agreement was obtained between simulated and observed water fluxes, and DFBA and *E. coli* concentrations at three sampling stations. Improved fit for *E. coli* BTCs can be obtained by prescribing its TS ratio parameter different from that found for DFBA conservative tracer.
3. The mass of the initially resuspended bacteria is not sufficient to support the concentrations found in water on later stages. Comparison of simulated and measured *E. coli* concentrations indicated that significant resuspension of *E. coli* continued when water flow returned to the base level after the water pulse passed and bottom shear stress was small.
4. Assuming that TS volumes are not related to the nature of the dissolved or suspended substance, then the TS volumes should be the same for the DFBA and *E. coli*, and some additional mechanisms exist that create elevated *E. coli* concentrations long after the water pulse passage. The mechanism of continued bacterial release from sediment could be due to an erosive boundary layer exchange enhanced by changes in biofilm properties via erosion and sloughing detachment. We speculated that this hypothesis might help in resolving discrepancies between TS volumes estimated for conservative tracer and bacteria transport.

Appendix A. Supplementary data

Supplementary data related to this article can be found at http://dx.doi.org/10.1016/j.watres.2013.02.011.

REFERENCES

Angier, J.T., McCarty, G.W., Prestegaard, K.L., 2005. Hydrology of a first-order riparian zone and stream, mid-Atlantic coastal plain, Maryland. Journal of Hydrology 309 (1–4), 149–166.

Alm, E.W., Burke, J., Spain, A., 2003. Fecal indicator bacteria are abundant in wet sand at freshwater beaches. Water Research 37, 3978–3982.

Alpkvist, E., Klapper, I., 2007. Description of mechanical response including detachment using a novel particle method of biofilm/flow interaction. Water Science & Technology 55, 265–273.

An, Y.-J., Kampbell, D.H., Breidenbach, J.P., 2002. *Escherichia coli* and total coliforms in water and sediments at lake marinas. Environmental Pollution 120, 771–778.

Arcement, G.J., Colson, B.E., Ming, C.O., 1979. Backwater at Bridges and Densely Wooded Flood Plains. Cypress Creek Near Downsville, Louisiana. US Geological Survey Hydrologic Investigations Atlas. HA-603, scales 1:62,500 and 1:2000, three sheets.

Atwill, R., Lewis, D., Pereira, M., Huerta, M., Bond, R., Ogata, S., Bass, P., 2007. Characterizing Freshwater Inflows and Sediment Reservoirs of Fecal Coliforms and E. Coli at Five

Estuaries in Northern California. University of California School of Veterinary Medicine and Cooperative Extension in Sonoma and Marin Counties, Davis, CA. http://ucce.ucdavis.edu/files/filelibrary/2161/41255. pdf (accessed 20.02.11).
Bai, S., Lung, W.S., 2005. Modeling sediment impact on the transport of fecal bacteria. Water Research 39 (20), 5232–5240.
Bear, J., 1979. Hydraulics of Groundwater. McGraw-Hill Book Co, London, p. 567.
Bencala, K.E., Walters, R.A., 1983. Simulation of solute transport in a mountain pool-and-riffle stream: a transient storage model. Water Resources Research 19, 718–724.
Biron, P., Robson, C., Lapointe, M.F., Gaskin, S.J., 2004. Comparing different methods of bed shear stress estimates in simple and complex flow fields. Earth Surface Processes and Landforms 29, 1403–1415.
Briggs, M.A., Gooseff, M.N., Arp, C.D., Baker, M.A., 2009. A method for estimating surface transient storage parameters for streams with concurrent hyporheic storage. Water Resources Research 45, W00D27. http://dx.doi.org/10.1029/2008WR006959.
Cardenas, M., Gailani, J., Ziegler, C.K., Lick, W., 1995. Sediment transport in the lower Saginaw River. Marine and Freshwater Research 46 (1), 337–347.
Chapra, S.C., 1997. Surface Water Quality Modeling. McGraw-Hill, New York.
Characklis, G., Dilts, M., Simmons, O., Likirdopulos, C., Krometis, L., Sobsey, M., 2005. Microbial partitioning to settleable particles in stormwater. Water Research 39, 1773–1782.
Cho, K.H., Pachepsky, Y.A., Kim, J.H., Guber, A.K., Shelton, D.R., Rowland, R., 2010. Release of Escherichia coli from the bottom sediment in a first-order creek: experiment and reach-specific modeling. Journal of Hydrology 391 (3–4), 322–332.
Chow, V.T., 1959. Open-channel Hydraulics. McGraw- Hill Book Co., New York, p. 680.
Collins, R., Rutherford, K., 2004. Modelling bacterial water quality in streams draining pastoral land. Water Research 38, 700–712.
Colson, B.E., Ming, C.O., Arcement, G.J., 1979. Backwater at Bridges and Densely Wooded Flood Plains, Yockanookany River Near Thomastown, Mississippi. US Geological Survey Hydrologic Investigations Atlas. HA-599, scales 1:62,500 and 1:8000, nine sheets.
Crabill, C., Donald, R., Snelling, J., Foust, R., Southam, G., 1999. The impact of sediment fecal coliform reservoirs on seasonal water quality in Oak Creek, Arizona. Water Research 33, 2163–2171.
Cunge, J., Holly, F., Verwey, A., 1980. Practical Aspects of Computational River Hydraulics. Pitmn Publsher Ltd.
Doyle, J.D., Tunnicliff, B., Kramer, K., Kuehl, R., Brickler, S.K., 1992. Instability of fecal coliform populations in waters and bottom sediments at recreational beaches in Arizona. Water Research 26, 979–988.
Droppo, I.G., Jaskot, C., Nelson, T., Milne, J., Charlton, M., 2007. Aquaculture waste sediment Stability: Implications for waste Migration. Water, Air & Soil Pollution 183 (1–4), 59–68.
Droppo, I.G., Liss, S.N., Williams, D., Nelson, T., Jaskot, C., Trapp, B., 2009. Dynamic existence of waterborne pathogens within river sediment compartments. Implications for water quality regulatory affairs. Environmental Science & Technology 43, 1737–1743.
Elmund, G.K., Allen, M.J., Rice, E.W., 1999. Comparison of *Escherichia coli*, total coliform, and fecal coliform populations as indicators of wastewater treatment efficiency. Water Environmental Research 71, 332–339.
England, R., 1969. Error estimates for Runge-Kutta type solutions to systems of ordinary differential equations. The Computer Journal 12, 166–170.
Ferguson, C.M., Coote, B.G., Ashbolt, N.J., Stevenson, I.M., 1996. Relationships between indicators, pathogens and water quality in an estuarine system. Water Research 30, 2045–2054.
Fries, J.S., Characklis, G.W., Noble, R.T., 2006. Attachment of fecal indicator bacteria to particles in the Neuse River Estuary. Journal of Environmental Engineering 132, 1338–1345.
Garzio, A., 2009. Survival of E. coli delivered with manure to stream sediment. Environmental Science and Policy Honors thesis. University of Maryland, College Park.
Garzio-Hadzick, A., Shelton, D.R., Hill, R.L., Pachepsky, Y.A., Guber, A.K., Rowland, R., 2010. Survival of manure-borne E. Coil in streambed sediment: effects of temperature and sediment properties. Water Research 44, 2753–2762.
Ge, Y., Boufadel, M.C., 2006. Solute transport in multiple-reach experiments: evaluation of parameters and reliability of prediction. Journal of Hydrology 323, 106–119.
Gee, G.W., Or, D., 2002. Particle size analysis. In: Dane, J., Topp, G.C. (Eds.), Methods of Soil Analysis. Part 4. Physical Methods. ASA and SSSA, Madison, WI, pp. 278–282.
Gerbersdorf, S.U., Jancke, T., Westrich, B., Paterson, D.M., 2008. Microbial stabilization of riverine sediments by extracellular polymeric substances. Geobiology 6 (1), 57–69.
Gooseff, M.N., Bencala, Kenneth E., Wondzell, S.M., 2008. Solute transport along stream and river networks. In: Rice, S.P., Roy, A.G., Rhoads, B.L. (Eds.), River Confluences, Tributaries and the Fluvial Network. JohnWiley & Sons, Ltd (Ch 18).
Goyal, S.M., Gerba, C.P., Melnick, G.L., 1977. Occurrence and distribution of bacterial indicators and pathogens in canal communities along the Texas Coast. Applied and Environmental Microbiology 34, 139–149.
Grant, S.B., Litton-Mueller, R.M., Ahn, J.H., 2011. Measuring and modeling the flux of fecal bacteria across the sediment-water interface in a turbulent stream. Water Resources Research 47, W05517. http://dx.doi.org/10.1029/2010WR009460.
Guber, A.K., Pachepsky, Y.A., Shelton, D.R., Yu, O., 2007. Effect of manure on fecal coliform attachment to soil and soil particles of different sizes. Applied and Environmental Microbiology 73, 3363–3370.
Haefner, F., Boy, S., Wagner, S., Behr, A., Piskarev, V., Palatnik, V., 1997. The 'front limitation' algorithm. A new and fast finite-difference method for groundwater pollution problems. Journal of Contaminant Hydrology 27, 43–61.
Harvey, J.W., Wagner, B.J., Bencala, K.E., 1996. Evaluating the reliability of the stream tracer approach to characterize stream-subsurface water exchange. Water Resources Research 32 (8), 2441–2451.
Hively, W.D., McCarty, G.W., Angier, J.T., Geohring, L.D., 2006. Weir design and calibration for stream monitoring in a riparian wetland. Hydrological Science and Technology 22, 71–82.
Jamieson, R., Gordon, R., Joy, D., Lee, H., 2004. Assessing microbial pollution of rural surface waters: a review of current watershed scale modeling approaches. Agricultural Water Management 70 (1), 1–17.
Jamieson, R.C., Joy, D.M., Lee, H., Kostaschuk, R., Gordon, R.J., 2005. Resuspension of sediment-associated Escherichia coli in a natural stream. Journal of Environmental Quality 34, 581–589.
Köhne, J.M., P.Mohanty, B., Šimůnek, J., 2005. Inverse dual-permeability modeling of preferential water flow in a soil column and implications for field-scale solute transport. Vadose Zone Journal 5, 59–76.
Kurganov, A., Petrova, G., 2008. A central-upwind scheme for nonlinear water waves generated by submarine landslides. Hyperbolic Problems: Theory, Numerics, Applications IV, 635–642.

Lau, Y.L., Droppo, I.G., 2000. Influence of antecedent conditions on critical shear stress of bed sediments. Water Research 34 (2), 663–667.
Lee, D.H., Bedford, K.W., Yen, C.J., 1994. Storm and entrainment effects on tributary sediment loads. Journal of Hydraulic Engineering 120 (1), 81–103.
Legates, D.R., McCabe Jr., G.J., 1999. Evaluating the use of "goodness-of-fit" measures in hydrologic and hydroclimatic model validation. Water Resources Research 35, 233–241.
McDonald, A., Kay, D., Jenkins, A., 1982. Generation of fecal and total coliform surges by stream flow manipulation in the absence of normal hydrometeorological stimuli. Applied and Environmental Microbiology 44, 292–300.
Muirhead, R.W., Davies-Colley, R.J., Donnison, A.M., Nagels, J.W., 2004. Fecal bacteria yields in artificial flood events: quantifying in-stream stores. Water Research 38, 1215–1224.
Olstadt, J., Schauer, J.J., Standridge, J., Kluender, S., 2007. A comparison of ten USEPA approved total coliform/*E. Coli* tests. Journal of Water and Health 5, 267–282.
Pachepsky, Y.A., Shelton, D.R., 2011. *Escherichia coli* and fecal coliforms in freshwater and estuarine sediments. Critical Reviews in Environmental Science and Technology 41 (12), 1067–1110.
Pachepsky, Ya.A., Sadeghi, A.M., Bradford, S.A., Shelton, D.R., Guber, A.K., Dao, T.H., 2006. Transport and fate of manure-borne pathogens: modeling perspective. Agricultural Water Management 86, 81–92.
Press, W.W., Teukolsky, S.A., Vetterling, W.T., Flannery, B.P., 1992. Numerical Recipes in Fortran: The Art of Scientific Computing, second ed. Cambridge University Press, New York.
Rehmann, C.R., Soupir, M.L., 2009. Importance of interactions between the water column and the sediment for microbial concentrations in streams. Water Research 43, 4579–4589.
Runkel, R.L., 2002. A new metric for determining the importance of transient storage. Journal of the North American Benthological Society 21, 529–543.
Runkel, R.L., Bencala, K.E., Kimball, B.A., 1999. Modeling solute transport and geochemistry in streams and rivers using OTIS and OTEQ. In: Morganwalp, D.W. (Ed.). In: Buxton, H.T. (Ed.), U.S. Geological Survey Toxic Substances Hydrology Program: Proc. of The Technical Meeting, Charleston, South Carolina, 8–12 March 1999, vol 1. Contamination from hardrock mining, pp. 120–127. U.S. Geological Survey Water-Resources Investigations Report 99-4018A.
Russo, A.R., Hunn, J., Characklis, G.W., 2011. Considering bacteria-sediment associations in microbial fate and transport modeling. Journal of Environmental Engineering 137 (8), 697–706.
Schlicting, H., 1987. Boundary Layer Theory, seventh ed. McGraw-Hill, New York.
Scott, D.T., Gooseff, M.N., Bencala, K.E., Runkel, R.L., 2003. Automated calibration of a stream solute transport model: implications for interpretation of biogeochemical parameters. Journal of the North American Benthological Society 22 (4), 492–510.
Smith, J., Edwards, J., Hilger, H., Steck, T.R., 2008. Sediment can be a reservoir for coliform bacteria released into streams. Journal of General and Applied Microbiology 54, 173–179.
Steets, B.M., Holden, P.A., 2003. A mechanistic model of runoff-associated fecal coliform fate and transport through a coastal lagoon. Water Research 37, 589–608.
Stoker, J.J., 1957. Water Waves. The Mathematical Theory with Applications. Interscience Publisher.
Stone, M., Emelko, M.B., Droppo, I.G., Silins, U., 2011. Biostabilization and erodibility of cohesive sediment deposits in wildfire-affected streams. Water Research 45, 521–534.
Tian, Y.Q., Gong, P., Radke, J.D., Scarborough, J., 2002. Spatial and temporal modeling of microbial contaminants on grazing farmlands. Journal of Environmental Quality 31 (3), 860–869.
US EPA, 1986. Ambient Water Quality Criteria for Bacterias-1986. EPA-440/5-84-002.
US EPA, 2003. Bacterial Water Quality Standards for Recreational Waters (Freshwater and Marine Water). US EPA EPA-823-R-03–008.
van Genuchten, M.T., Alves, W.J., 1982. Analytical Solutions of the One-dimensional Convective-dispersive Solute Transport Equation. USDA ARS Technical Bulletin Number 1661. U.S. Salinity Laboratory Riverside.
Wade, T.J., Calderon, R.L., Sams, E., Beach, M., Brenner, K.P., Williams, A.H., Dufour, A.P., 2006. Rapidly measured indicators of recreational water quality are predictive of swimming-associated gastrointestinal illness. Environmental Health Perspectives 114, 24–28.
Wallis, S.G., Manson, J.R., 2004. Methods for predicting dispersion coefficients in rivers. Water Management 157, 131–141.
Wilkinson, R.J., Kay, D., Wyer, M., Jenkins, A., 2006. Processes driving the episodic flux of faecal indicator organisms in streams impacting on recreational and shellfish harvesting waters. Water Research 40, 153–161.
Yang, L., Lin, B., Falconer, R.A., 2008. Modelling enteric bacteria level in coastal and estuarine waters. Engineering and Computational Mechanics 161, 179–186.